Research of antibacterial activity on silver containing yttria-stabilized–zirconia bioceramic

Shih-Fu Ou[a,b,c], Mao-Suan Huang[a,d,e], Shi-Yung Chiou[b], Keng-Liang Ou[a,c,f],*

[a]Research Center for Biomedical Devices and Prototyping Production, Taipei Medical University, Taipei 110, Taiwan
[b]Institute of Mold & Die Engineering, National Kaohsiung University of Applied Sciences, Kaohsiung 807, Taiwan
[c]Graduate Institute of Biomedical Materials and Tissue Engineering, Taipei Medical University, Taipei 110, Taiwan
[d]Department of Oral Hygiene, College of Oral Medicine, Taipei Medical University, Taipei, Taiwan
[e]Department of Dentistry, Taipei Medical University-Shuang Ho Hospital, Taipei 235, Taiwan
[f]Research Center for Biomedical Implants and Microsurgery Devices, Taipei Medical University, Taipei 110, Taiwan

Abstract

An antibacterial bioceramic, silver containing yttria-stabilized zirconia (YSZ), was fabricated by sintering for dental prosthesis applications. The biocompatibility, hemocompatibility and antibacterial ability of the silver containing YSZ were evaluated. The addition of silver did not cause tetragonal phase to transform into monoclinic phase and the silver containing YSZ maintained an excellent mechanical property. Furthermore, the sintered silver containing YSZ showed no toxicity and possessed a good antibacterial ability against both *Staphylococcus aureus* (*S. aureus*) and *Escherichia coli* (*E. coli*) cell.
© 2012 Elsevier Ltd and Techna Group S.r.l. All rights reserved.

Keywords: Antibacterial bioceramic; Yttria-stabilized zirconia; Biocompatibility

1. Introduction

In 1969, zirconia was first proposed to be used in orthopedic application especially for replacing the hip head due to its superior mechanical properties [1]. Since 1990, zirconia has been confirmed to possess no cytotoxicity and create less inflammation reaction compared to titanium [2–5]. Based on the aesthetic point of view, the dental research towards metal-free prosthetic restorations in order to maintain the color of soft tissue resembling the natural one [6]. Recently, zirconia based ceramic system has been successfully used in restorative and prosthetic density due to its high flexural strength and fracture toughness [7–9] and its color is similar to tooth color [10]. Two possible failures of zirconia implant are considered as mechanical fracture and biological infection of the

peri-implant tissues [11–14]. The fracture toughness of zirconia can be improved by alloying zirconia with Y_2O_3 and the yittra stabilized zirconia was named YSZ [15,16]. The toughening mechanism of YSZ is based on crack-tip shielding under compressive stresses associated with tetragonal zirconia transform into the monoclinic phase with an increase in volume [17].

However, YSZ does not possess the properties to protect against bacterial adhesion or infection. Bacterial adhesion to implant surfaces is a major source of inflammation and infection. When bacterial adhesion occurs on implant surfaces, it is very difficult to be clinically treated because of the formation of bacterial biofilms, which can obstruct the immune response, systemic antibiotic therapy, and the integration of the indwelling implants with the surrounding tissue [13]. Hence, it is necessary to develop an antibacterial YSZ ceramic by adding various active antibacterial agents to combat biofilm formation, without sacrificing any useful mechanical or biological properties.

It is well known that Ag ions and Ag-based compounds can effectively destroy the cell walls and cell membranes of

---

*Corresponding author at: Graduate Institute of Biomedical Materials and Tissue Engineering, Taipei Medical University, Taipei 110, Taiwan. Tel.: +886 2 27361661x5100; fax: +886 2 27395524.
E-mail address: klou@tmu.edu.tw (K.-L. Ou).

bacteria to inhibit their growth [18,19]. Furthermore, Ag possess a suitable biocompatibility because of its remarkably low human toxicity compared to other heavy metal ions. [20]. In recent year, the chemical reduction technique has been used to fabricate Ag particles and Ag incorporating coating; however, it is a long time procedure and produce pollutant solution [21]. Therefore the aim of the present study was to develop an antibacterial ceramic by co-sintering Ag and YSZ nanoparticles. This study further investigated the microstructural characteristics and mechanical properties of YSZ–Ag ceramic sintered at varying temperature. In addition, the biocompatibility, hemocompatibility and antibacterial ability were evaluated.

2. Materials and methods

2.1. Sample preparation

ZrO$_2$ powder partially stabilized by 3 mol% Y$_2$O$_3$ (YSZ) was used in this study. The YSZ powder was mixed with 5 wt% silver powder (commercially available). Then the mixed powder was pressed in a stainless steel mould (10 mm in diameter) under a hydraulic pressure of 300 MPa for 1 min. Pressing was followed by the consolidation of the green compacts by ambient pressure sintering performed in air using a furnace. All samples were heated at the following temperatures: 1100, 1200, 1300 and 1400 °C for 1 h, with a ramp rate of 5 °C/min. The same rate was also followed up to 500 °C during cooling. After sintering, the properties of interest were characterized for each compact. In this study, the Ag containing YSZ sintered compact was named YSZ–Ag. And the YSZ–Ag sintered at 1100, 1200, 1300 and 1400 °C were denoted as YSZ–Ag-1, YSZ–Ag-2, YSZ–Ag-3 and YSZ–Ag-4, respectively.

2.2. Characterizations of sintered samples

The sintering temperature was optimized based on the sintered density of the samples. The relative density of the compacts was measured by the Archimedes' method. The Vickers' hardness of the compacts was measured by using a hardness tester (MVK-H1, Meter-Mitutoyo, Japan). Indentations were performed on polished surfaces at a test load of 300 N with an indentation time of 15 s. In this study, six samples for each sintering process were performed to obtain an average relative density and hardness.

The phases of the sintered compacts were characterized by X-ray diffractometry (XRD) (Model 2200, Rigaku Co., Tokyo, Japan). Monochromatic Cu K_α radiation was used at operating values of 40 kV and 30 mA. The XRD data were collected over the 2θ range of 20–40° at a step size of 0.04°/step and a count time of 5 s. The microstructure was examined using scanning electron microscopy (SEM; Model JSM, JEOL Co., Tokyo, Japan) and transmission electron microscopy (TEM; Model JEM2100, JEOL Co., Tokyo, Japan).

2.3. Cell culture

YSZ and YSZ–Ag specimens were placed into a 24-well polystyrene plate. Before cell culturing, all the specimens were shined by ultraviolet ray (UV) for 24 h. The test specimens were sterilized and washed several times with Dulbecco's modified Eagle's medium (DMEM, Gibco) and phosphate-buffered saline (PBS, 0.1 M, pH 7.2). The culture medium consisted of DMEM containing 10% fetal bovine serum (FBS), 100 μg/ml of streptomycin, and 100 units/ml of penicillin.

The L929 cell suspension with a density of 1×10^4 cells/ml was added into the culture well. 500 ml culture solution and 50 μl 3-[4,5-dimethylthiazol-2-y1]-2,5-diphenyltetrazo-lim bromide (MTT) label solution were added into every culture well before placing the plate inside a culture chamber at 37 °C in a humidified atmosphere of 95% air and 5% CO$_2$. The culture medium was changed every three days. The test specimens were cultured for various periods of time, i.e., 8 h, 24 h, 72 h, 120 h, 168 h and 216 h. The proliferation behavior was determined by performing MTT assay to obtain the cell optical density (OD) by the plate reader (ELISA, DYNEX-MRX II) at $\lambda = 595$ nm.

2.4. Antibacterial activity test

The antibacterial procedure was following the Japan Industrial Standard (JIS) Z2801:2010 specifications. The tests were performed by using bacteria containing solutions (suspensions) held in close contact with test surfaces. The bacterial strains, Gram-positive *Staphylococcus aureus* (*S. aureus*) ATC C6538P, and Gram-negative *Escherichia coli* (*E. coli*) ATCC8739 were used as test organisms in the test. Before examination, the specimens and experimental tools were sterilized at 121 °C for 15 min by autoclaving. Single colonies were incubated in a nutrition broth (Difco 234000, USA) and the initial bacterial suspensions were prepared at 4×10^5 cfu ml^{-1}. Subsequently, the bacterial suspension (400 μl) was spread on specimens and incubated at 37 °C for 24 h. After incubation, the bacterial suspension on the specimens was washed into a centrifuge tube (Crystalgen, 50 ml) by using 2 ml buffer solution (Invitrogen, GIBCO pH 7.4). A serial dilution of the corresponding specimens using the dilute buffer was performed to concentrations of 10^0, 10^1, 10^2, 10^3 and 10^4 fold. Then, these diluted bacterial suspensions were pipetted (100 μl) onto nutrition agar (Difco 214530, USA) plates with a streaked out loop and grown overnight at 37 °C. The number of viable cells was determined by counting the number of bacterial colonies that grew in each Petri dish. The antibacterial rate (AR) was determined using following equation according to JIS

Z2801:2010 specifications,

$$AR(\%) = 100 \times [N_{(control)} - N_{(sample)}]/N_{(control)} \qquad (1)$$

where N(control) is the number of bacteria adhering to the Ag-free specimens after a 24 h incubation period, and N(sample) is the number of bacteria adhering to the Ag-containing specimens after incubation for 24 h.

3. Results and discussion

3.1. Microstructural evaluation

The ZrO_2 particles with the size of 70 to 120 nm were shown in Fig. 1(a). Fig. 1(b) shows the TEM micrograph of Ag particles and the size between 100 and 500 nm.

Fig. 2 shows the XRD patterns of the YSZ–Ag compact sintered at various temperatures. The XRD patterns associated with tetragonal YSZ and no monoclinic phase were observed. Comparing all samples, only a slight difference in the full width at half maximum of principal reflection (1 1 1) was found. It suggested that raising temperature is beneficial for grain growth.

Fig. 3(a)–(d) show the surface morphology of the YSZ–Ag-1, YSZ–Ag-2, YSZ–Ag-3 and YSZ–Ag-4, respectively. Obviously, a great numbers of pores resided in the compact when the compact was sintered at 1100 °C as

Fig. 1. The TEM micrographs of (a) ZrO_2 particles and (b) Ag particles.
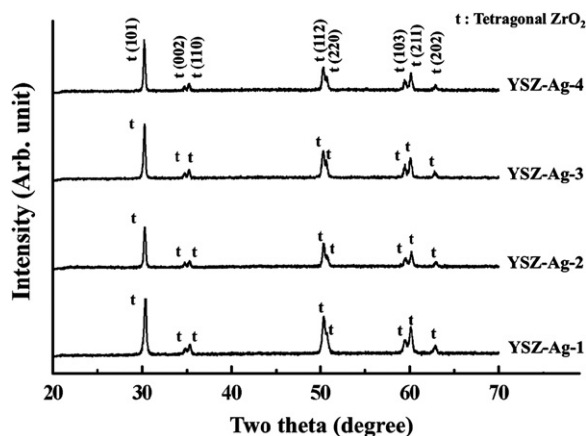

Fig. 2. The XRD patterns of the YSZ–Ag compacts sintered at various temperatures.

shown in Fig. 3. The grain consisting of nano-particles was observed in upper right corner of Fig. 3. The grain size increased while population density of pores decreased as the temperature increased to 1200 °C (Fig. 3(b)). Above 1300 °C sintering, the grains compactly contacted to each other and the pores were greatly eliminated. With regard to the grain size, a typical sintering phenomenon, the grain size increases while the porosity decreases with raising the sintering temperature, was recognized in Fig. 3.

3.2. Densification studies

In this study, the relative density was presented as a percentage of the theoretical density by assuming a theoretical density of ZrO_2. Fig. 4 shows the effect of sintering temperature on the grain size and the relative density. The relative density of the YSZ–Ag compact increased with temperature to the maximum of 95% at 1400 °C.

Densification is a process of eliminating the pores along the grain boundaries that were introduced during green compact fabrication. During the initial sintering, grain boundaries moved faster than pores, so isolated pores remained within the grain interior. Although pores could be moved by surface diffusion, this is hard to achieve, so the maximum density was limited.

Fig. 4 also shows the average grain size of the YSZ–Ag compacts as a function of sintering temperature. In the beginning, the grains slowly grew with temperature between 1100 and 1200 °C. Generally, the rate of grain growth depends on the densification of the sintered compact. For instance, during the initial sintering period, the pores were induced during green compact fabrication and the pores can inhibit grain boundary migration, since they exist along grain boundaries [22]. However, because grain boundary migrates faster than the pores, the pores gradually transform into the isolated pores within grains with raising temperature. Consequently, the extent of the pinning of pores at grain boundaries would decrease at a high temperature. Thus, it resulted in an accelerated grain
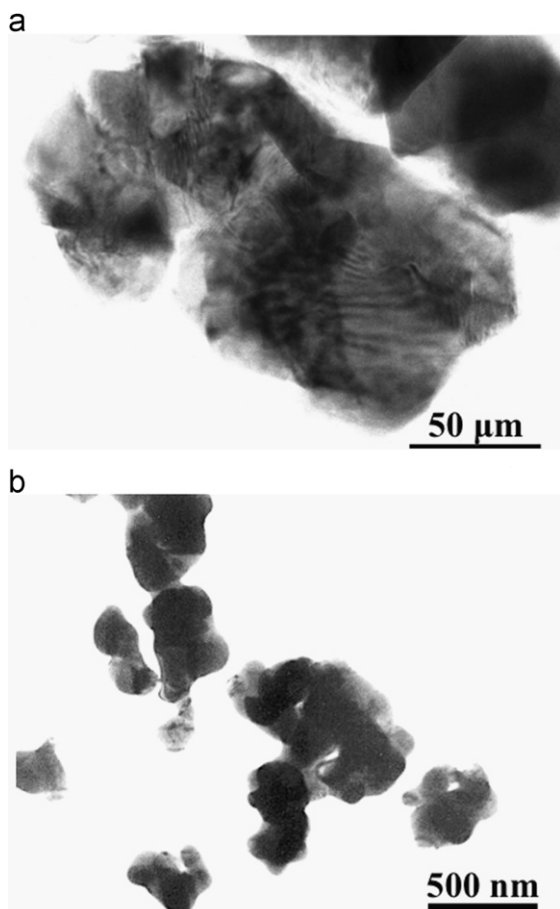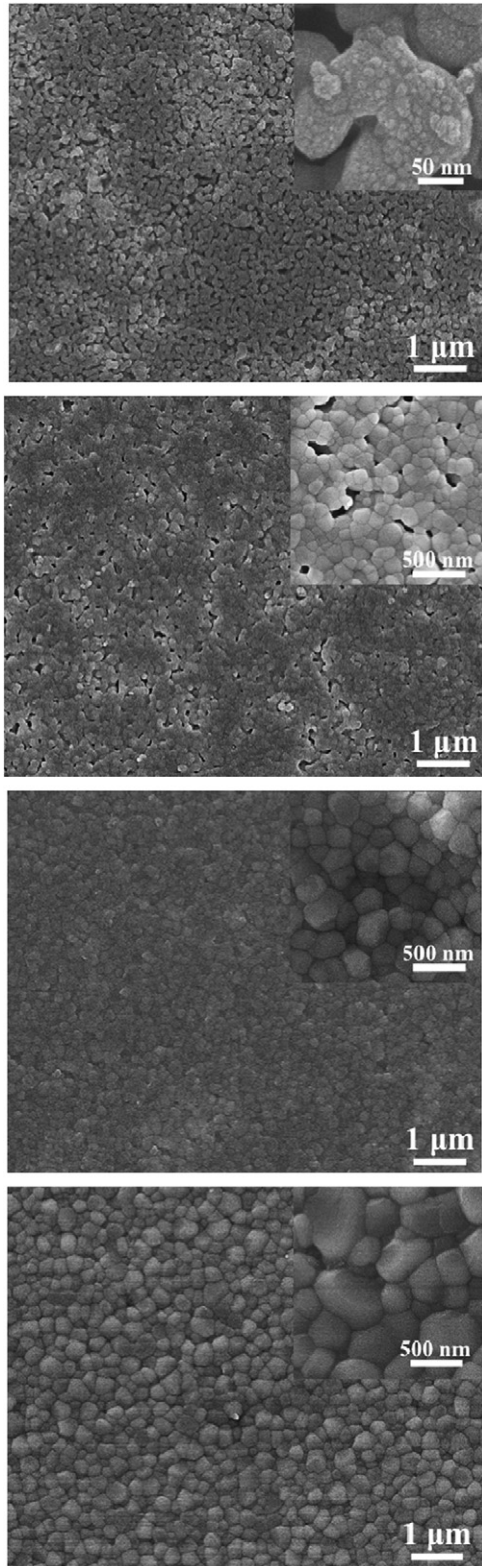
Fig. 3. The SEM micrographs of the YSZ–Ag compacts sintered at (a) 1100, (b) 1200, (c) 1300 and (d) 1400 °C.
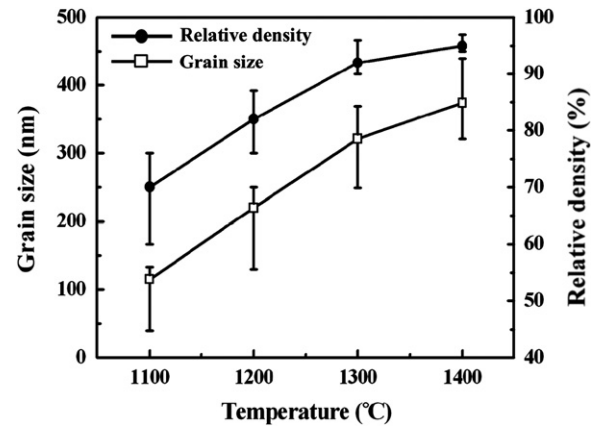

Fig. 4. The grain size and relative density of the YSZ–Ag compacts as a function of temperature.
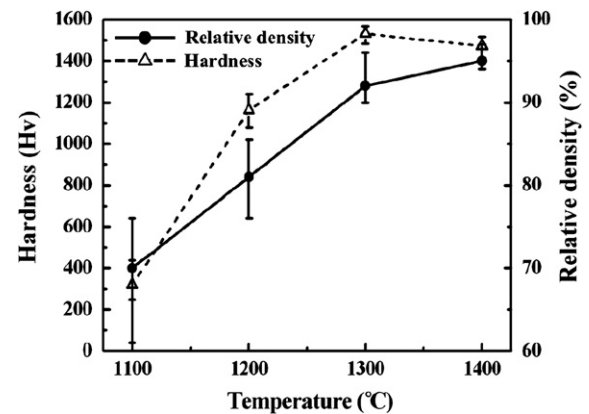
Fig. 5. The hardness and relative density of the YSZ–Ag compacts as a function of temperature.

growth, which occurred at 1300 °C in this study as shown in Fig. 4.

Fig. 5 shows the hardness and relative density of the YSZ–Ag compacts as a function of sintering temperature. The hardness of the YSZ–Ag compacts increased with the temperature to the maximum hardness of 1460 Hv at 1300 °C and followed by maintained constant as the temperature increased to 1400 °C.

The mechanical properties of YSZ–Ag compact generally varied with the sintering temperature and depended on the density and grain size. In the present study, at low temperature (< 1200 °C), the relatively low hardness obtained is mainly attributed to a relatively low bulk density of the sintered compact. The hardness shows similar trend as the relative density, suggesting the strengthening of the sintered compact is directly related to the densification of the sintered compact. On the other hand, after 1300 °C, the reason for an insignificant decline in hardness is due to grain growth.

3.3. In vitro tests

ZrO_2 and YSZ have been demonstrated to be not cytotoxic in the literature [23–25]. In the present study, the biocompatibility of Ag contained YSZ was evaluated by culturing L929 cell line on the YSZ–Ag compact sintered at 1400 °C (specimen YSZ–Ag-4). And the in vitro results show that the YSZ–Ag-4 compact

possessed a similar biocompatibility and as the YSZ compact and control specimen, as shown in Fig. 6.

Table 1 lists the antibacterial rate of the YSZ and YSZ–Ag-4 compact. The YSZ did not have antibacterial ability; in contrast, YSZ–Ag-4 displayed excellent antibacterial ability against *S. aureus* and *E. coli*. In our previous study [14], the antibacterial mechanism of Ag-containing stainless steel has been clarified and the released Ag ions were considered as the main agent to attack bacteria. In the present study, Ag ions were also detected in the bacterial suspension of YSZ–Ag-4 compact by the inductively coupled plasma mass spectrometer. Consequently, the antibacterial mechanism of Ag-containing YSZ is considered as following steps: the released Ag ions were absorbed into the surfaces of negatively charged bacterial cell walls because of the electrostatic attraction between negatively charged bacterial cells and positively charged Ag ions [26]. Furthermore, the Ag ions destroy the cell walls and cell membranes. When the Ag ions combined with the bacterial DNA by penetrating the cell walls, they caused bacterial degeneration and inhibited cells to replicate [27].

In addition, the results of antibacterial activity indicated that the YSZ–Ag-4 shows a better antibacterial ability against *S. aureus* than against *E. coli*. The resistant ability of bacterial strain depends on the sensitivity and the structure of the outer membrane of bacteria. Ag ions have demonstrated to have a lower sensitive to the Gram-negative bacteria. Moreover, the outer membrane of Gram-negative bacteria provided an efficient resistant barrier because the outer membrane comprised tightly packed lipopolysaccharide molecules [28,29].

In order to observe the distribution of bacterial, the bacteria suspension cultured on the YSZ and YSZ–Ag-4 was dropped onto carbon tape. For the YSZ specimen, a great number of *E. coli* aggregations and the biofilm covering on the surface were observed in Fig. 7(a). However, with respect to YSZ–Ag-4, only few *E. coli* were observed, as shown in Fig. 7(b), and no biofilm was observed. It suggests that Ag can effectively inhibit bacteria from adhering on the surface, which is also observed on the Ag–Pd alloy surface [30].

To sum up, the Ag containing YSZ compact with advantageous antibacterial properties against both *E. coli* and *S. aureus* is attributed to 0.5 wt% Ag addition. The Ag-containing YSZ compact can be considered as an antibacterial metal candidate for use as a biomaterial use.

4. Conclusions

This study fabricated an antibacterial bioceramic by co-sintering silver and YSZ powder with nano-size.
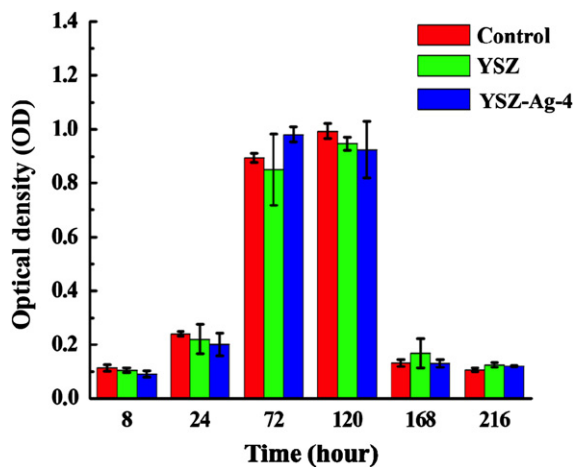

Fig. 6. Variation in optical density of cell culture as a function of culturing time.

Table 1
The antibacterial rate of the YSZ and YSZ–Ag-4 specimen.

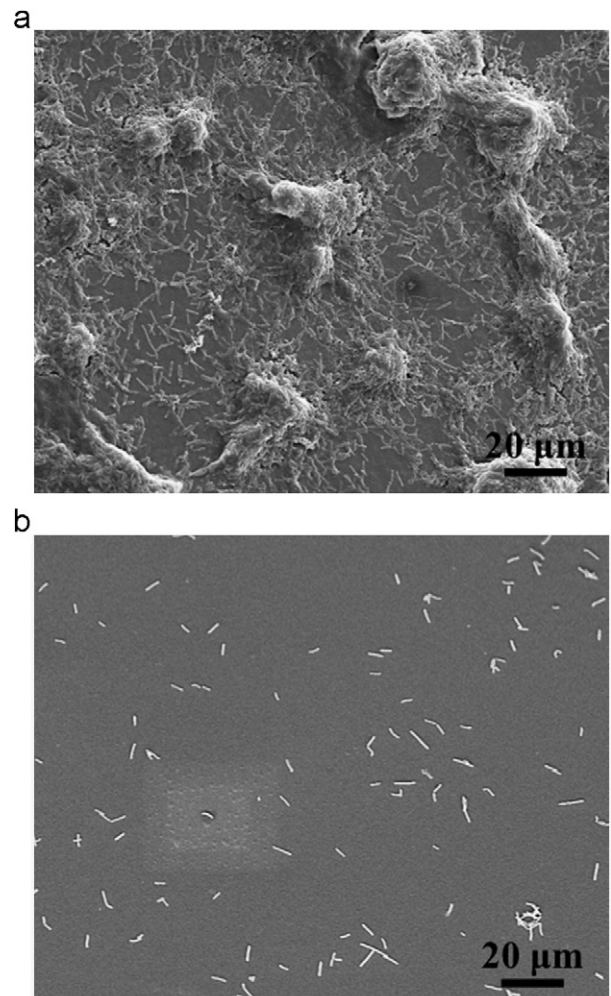| Specimen	S. aureus (%)	E. coli (%)
YSZ	0	0
YSZ–Ag-4	98.6	87.9

Fig. 7. The SEM micrographs of *E. coli* cultured in the (a) suspension of YSZ and (b) suspension of YSZ–Ag-4 after 24 h incubation.

The biocompatibility and antibacterial properties of Ag containing YSZ were evaluated. As the sintering temperature increased from 1100 to 1400 °C, a decrease of porosity, an increase of density and an increase of hardness were observed. Adding Ag did not result in tetragonal phase transforming into monoclinic phase and hence the silver containing YSZ maintained excellent mechanical properties. In addition, the Ag containing YSZ exhibited biocompatibility. The Ag containing YSZ behaved as excellent antibacterial agent against *S. aureus* and *E. coli* cell by releasing Ag ions to destroy and penetrate the cell wall which resulted in death of the cell.

References

[1] P.F. Manicone, P.R. Iommetti, L. Raffaelli, An overview of zirconia ceramics: basic properties and clinical applications, Journal of Dentistry 35 (2007) 819–826.

[2] I. Dion, L. Bordenave, F. Lefebvre, R. Bareille, C. Baquey, J.-R. Monties, P. Havlik, Physico-chemistry and cytotoxicity of ceramics, Journal of Materials Science: Materials in Medicine 5 (1) (1994) 18–24.

[3] P. Torricelli, E. Verné, C.V. Brovarone, P. Appendino, F. Rustichelli, A. Krajewski, A. Ravaglioli, G. Pierini, M. Fini, G. Giavaresi, R. Giardino, Biological glass coating on ceramic materials: in vitro evaluation using primary osteoblast cultures from healthy and osteopenic rat bone, Biomaterials 22 (18) (2001) 2535–2543.

[4] C.H. Lohmann, D.D. Dean, G. Köster, D. Casasola, G.H. Buchhorn, U. Fink, Z. Schwartz, B.D. Boyan, Ceramic and PMMA particles differentially affect osteoblast phenotype, Biomaterials 23 (8) (2002) 1855–1863.

[5] H. Warashina, S. Sakano, S. Kitamura, K.-I. Yamauchi, J. Yamaguchi, N. Ishiguro, Y. Hasegawa, Biological reaction to alumina, zirconia, titanium and polyethylene particles implanted onto murine calvaria, Biomaterials 24 (21) (2003) 3655–3661.

[6] A.J. Raigrodski, Contemporary materials and technologies for all-ceramic fixed partial dentures: a review of the literature, The Journal of Prosthetic Dentistry 92 (6) (2004) 557–562.

[7] R.H.J. Hannink, P.M. Kelly, B.C. Muddle, Transformation toughening in zirconia-containing ceramics, Journal of the American Ceramic Society 83 (3) (2000) 461–487.

[8] J. Fischer, B. Stawarczyk, Compatibility of machined Ce-TZP/Al2O3 nano.composite and a veneering ceramic, Dental Materials 23 (12) (2007) 1500–1505.

[9] M.N. Aboushelib, C.J. Kleverlaan, A.J. Feilzer, Evaluation of a high fracture toughness composite ceramic for dental applications, Journal of Prosthodontics 17 (7) (2008) 538–544.

[10] C. Piconi, G. Maccauro, Zirconia as a ceramic biomaterial, Biomaterials 20 (1) (1999) 1–25.

[11] E.M.C.X. Lima, H. Koo, A.M.Vacca. Smith, P.L. Rosalen, A.A. Del.Bel. Cury, Adsorption of salivary and serum proteins, and bacterial adherence on titanium and zirconia ceramic surfaces, Clinical Oral Implants Research 19 (8) (2008) 780–785.

[12] S. Nasser, Prevention and treatment of sepsis in total hip replacement surgery, The Orthopedic clinics of North America 23 (2) (1992) 265–277.

[13] E.M. Hetrick, M.H. Schoenfisch, Reducing implant-related infections: active release strategies, Chemical Society Reviews 35 (9) (2006) 780–789.

[14] C.-F. Huang, H.-J. Chiang, W.-C. Lana, H.-H. Chou, K.-L. Ou, C.-H. Yu, Development of silver-containing austenite antibacterial stainless steels for biomedical applications part I: Microstructure characteristics, mechanical properties and antibacterial mechanisms, Biofouling 27 (5) (2011) 449–457.

[15] J. Chevalier, S. Deville, E. Münch, R. Jullian, F. Lair, Critical effect of cubic phase on aging in 3 mol% yttria-stabilized zirconia ceramics for hip replacement prosthesis, Biomaterials 25 (24) (2004) 5539–5545.

[16] S. Deville, L. Gremillard, J. Chevalier, G. Fantozzi, A critical comparison of methods for the determination of the aging sensitivity in biomedical grade yttria-stabilized zirconia, Journal of Biomedical Materials Research Part B: Applied Biomaterials 72B (2) (2005) 239–245.

[17] A.R. Studart, F. Filser, P. Kocher, L.J. Gauckler, Fatigue of zirconia under cyclic loading in water and its implications for the design of dental bridges, Dental Materials 23 (1) (2007) 106–114.

[18] R.M. Slawson, M.I. VanDyke, H. Lee, J.T. Trevors, Germanium and silver resistance, accumulation, and toxicity in microorganisms, Plasmid 27 (1) (1992) 72–79.

[19] Z.G.,.S.E. Stevens, Multiple parameters for the comprehensive evaluation of the susceptibility of *Escherichia coli* to the silver ion., Biometals 114 (1998) 27–32.

[20] J.L. Clement, P.S. Jarrett, Antibacterial silver, Metal Based Drugs 1 (5–6) (1994) 467–482.

[21] K. Xu, Y. Liu, S. Liu, A. Liu, P. Liu, L. Liu, L. Li, Microorganism adhesion inhibited by silver doped yttria-stabilized zirconia ceramics, Ceramic International 37 (2011) 2109–2115.

[22] M. Mazaheri, A.M. Zahedi, S.K. Sadrnezhaad, Two-step sintering of nanocrystalline ZnO compacts: effect of temperature on densification and grain growth, Journal of the American Ceramic Society 91 (1) (2008) 56–63.

[23] R.C. Garvie, C. Urbani, D.R. Kennedy, J.C. McNeuer, Biocompatibility of magnesia-partially stabilized zirconia (Mg-PSZ) ceramics, Journal of Materials Science: Materials in Medicine 19 (10) (1984) 3224–3228.

[24] P.C,M. G, Zirconia as a ceramic biomaterial, Biomaterials 20 (1) (1999) 1–25.

[25] M. Uo, G. Sjoren, A. Sundh, F. Watari, M. Bergman, U. Lerner, Cytotoxicity and bonding property of dental ceramics, Dental Materials 19 (6) (2003) 487–492.

[26] Y.S. Lin, R.D. Vidic, J.E. Stout, V.L. Yu, Negative effect of high pH on biocidal efficacy of copper and silver ions in controlling, Applied and environmental microbiology 68 (6) (2002) 2711–2715.

[27] Q.L. Feng, J. Wu, G.Q. Chen, F.Z. Cui, T.N. Kim, J.O. Kim, A mechanistic study of the antibacterial effect of silver ions on *Escherichia coli* and *Staphylococcus aureus*, Journal of Biomedical Materials Research 52 (4) (2000) 662–668.

[28] Niv Papo, S. Yechiel, A molecular mechanism for lipopolysaccharide protection of Gram-negative bacteria from antimicrobial peptides, Journal of Biological Chemistry 280 (2005) 10378–10387.

[29] K.-Y. Yoon, B.J. Hoon, J.H. Park, J. Hwang, Susceptibility constants of *Escherichia coli* and *Bacillus subtilis* to silver and copper nanoparticles, Science of the Total Environment 373 (2–3) (2007) 572–575.

[30] W.C. Chiang, C. Schroll, L.R. Hilbert, P. Møller, N.T. Tolker, Silver-Palladium surfaces inhibit biofilm formation, Applied and Environmental Mirobiology 75 (6) (2009) 1674–1678.